Copyright Notice

©2012 IEEE. Personal use of this material is permitted. However, permission to reprint/republish this material for advertising or promotional purposes or for creating new collective works for resale or redistribution to servers or lists, or to reuse any copyrighted component of this work in other works must be obtained from the IEEE.

Bayesian Train Localization Method Extended By 3D Geometric Railway Track Observations From Inertial Sensors

Oliver Heirich, Patrick Robertson, Adrián Cardalda García, Thomas Strang
DLR (German Aerospace Center)
Institute of Communications and Navigation
82234 Wessling, Germany
{firstname.lastname}@dlr.de

***Abstract*—The localization of trains in a railway network is necessary for train control or applications like autonomous train driving or collision avoidance systems. Train localization is safety critical and therefore the approach requires a robust, accurate and track selective localization. The proposed approach focuses on an onboard localization system using appropriate onboard sensors without any additional railway infrastructure. Global navigation satellite systems (GNSS) are very beneficial for this task, but the accuracy, measurement errors and the lack of availability in parts of the railway environment do not fulfill the requirements for a safety critical railway system. An inertial measurement unit (IMU) is used to increase robustness and accuracy, by sensing the position related effects of 3D track geometry on the train. In order to cope with multiple sensors, position related uncertainties and sensor errors, we propose a probabilistic approach with a Bayesian filter. In this paper we present a train localization approach using a particle filter in combination with multiple onboard train sensor measurements and a known track map. The particle filter estimates a topological position directly in the track map. First simulations show encouraging results in robustness and accuracy in critical railway scenarios.**

I. Introduction

Train localization systems are required for general train control, automatic train driving or collision avoidance. Current developments of collision avoidance systems for trains, such as RCAS[1] [1] require a robust and precise localization solution.

Train localization can either be achieved by onboard sensors [2]–[4], or sensors with additional infrastructure in the railway environment, such as balises on tracks [5]. We focus on the onboard train localization method, where sensor data is combined with a track map and a train motion model. Onboard train sensors are global navigation satellite system (GNSS) receivers, inertial measurement units (IMU), odometry and railway feature classification sensors [4], [6].

In contrast to map matching methods [2], [3], [7], our approach is based on a particle filter, which contains the map in the transition model and spreads particles exclusively in the topological domain.

A critical scenario for train localization is passing a switch with continued long stretches of parallel tracks. As GNSS position observations are not sufficient to guarantee a robust and accurate topological train position in all track network scenarios, inertial sensor data is applied. Opposed to known aiding techniques for combining GNSS and integrated inertial data to estimate a geographic position [8], we use inertial data to estimate a position directly on the track map. The track geometry affects the train accelerations and turn rates while the train is moving, because of the strong coupling of track and train. These accelerations and turn rates are measured by the IMU and compared with the stored track geometry from the digital map by a sequential Bayesian filter.

[1]Railway Collision Avoidance System, http://www.collision-avoidance.org

II. Train Localization

The goal of train localization is to estimate the train position in the track network by topological coordinates. This topological position is defined by a unique track ID R and a track length variable s. The origin of that length has to be defined for direction dir of the train related to the track. A positive direction points away from the origin, a negative towards the origin. The topological pose is a triplet of track ID, length and direction and defines the train position and attitude in topological coordinates unambiguously:

$$\mathrm{P}^{\mathrm{topo}} = \{R, s, dir\}. \tag{1}$$

The challenge of a train localization is a reliable track selective localization in scenarios where parallel tracks are interconnected by switches.

A. Onboard localization sensors

1) Global Navigation Satellite System (GNSS): Satellite navigation allows the determination of absolute positions in the geographic coordinate system without additional sensors and special prior knowledge about the actual position. The two main drawbacks of GNSS for railways are limited availability and relative low accuracy. An ideal condition for GNSS positioning is a direct line of sight from the antenna to the available satellites with no other objects in the vicinity. In the railways environment, this condition is not given in tunnels, below bridges and station roofs and in dense forests where signals are blocked. In these scenarios, GNSS positioning may not be available or at least has a decreased accuracy due to the disadvantageous constellation of the visible satellites. The accuracy is also reduced by multipath effects which may be present and constant over long distances. The railways environment contains a large amount of metallic structure such as tracks and power lines and the receiving antenna will be in

proximity to buildings, trees and other obstacles close to the track. A robust and precise localization can not be achieved by using GNSS only. A critical but frequent railways localization problem is the presence of parallel tracks. The distances of parallel tracks are $4-5\mathrm{m}$ [9] which is below the typical GNSS accuracy [10]. The limited availability of GNSS, the accuracy and the inability to measure in the topological domain do not cover the demands for a safety-of-life train localization required in systems such as collision avoidance.

2) Inertial Measurement Unit (IMU): An advantageous and complementary sensor for train localization is an inertial measurement unit (IMU). It combines the measurement of 6 different sensors by measuring three-dimensional translative accelerations and three-dimensional rotation turn rates of the train. The IMU provides continued data at a certain frequency. Inertial measurements suffer from errors such as sensor biases which are not constant over time and called drift. One conventional approach is the computation of attitude, speed and position [8] of a train. Therefore, the measurements are integrated once or twice. The drift causes high errors in the results because the errors sum up in every integration step. A different approach to apply an IMU is the measurement of the track's effects on the pose of the train. In previous work [11] we analyzed the position dependent geometric track characteristics measured by an IMU while the train is moving. The track geometry curvature, bank, bank change, slope and slope change of all track positions are stored in a digital map. A sequential Bayesian filter compares measurements with train positions with known geometry by likelihood functions. As a result, the best matching positions in the track network can be derived. The big advantage of that method is the lack of integrations.

3) Odometer: The odometer measures relative distance and velocity of the train, by counting wheel increments and measuring the period. Odometers suffer from errors of the velocity or relative distance measurements due to wheel slip in acceleration and deceleration phases and due to a changing wheel radius of worn tread [12]. Doppler radars for trains provide information about train velocity and displacement based on a different sensing method and errors occur due to different track bed conditions. When integrating the velocity to get distance estimates, these errors are cumulative.

4) Feature classification sensors: Feature sensors measure and classify a specific high-level characteristic of the railway environment. A position can be derived in combination with feature information from the digital map. An important feature sensor is the switch detector, which is able to recognize switches. These detectors are often augmented with a switch way detector, which determines the travel direction towards the switch and the track way. Other classifiers may recognize parallel tracks, platforms, station roofs, railway signs and signals, power masts, bridges or tunnel entrances. These feature sensors can be based on a camera vision sensor [6] or a magnetic eddy current sensor [4]. An eddy current sensor works as a metal detector and senses changes in the metallic structure of the tracks with its coils. These changes occur also in a switch and cause significant signal patterns while the train moves over a switch.

B. Coordinate Frames

For the correct computation of the train position estimate, different frame definitions are helpful:

*1) **Earth Frame**:* Absolute geographic positions for a train or a map point is defined in the earth frame. The coordinate systems we use for the earth frame are WGS84 latitude, longitude, altitude (LLA) coordinates or Cartesian earth-centered-earth-fixed (ECEF) coordinates.

*2) **Navigation Frame**:* The navigation frame is defined by the Cartesian north-east-down (NED) system. This frame spans an orthogonal plane to the gravity vector at a geographic position and allows position computations in the vicinity of the train or track position. A conversion from LLA to NED frame $C_{\text{earth}}^{\text{nav}}$ is found in [10].

*3) **Track Frame**:* We propose two types of track frames. The first is the **topological** coordinate frame with tracks, track positions and a direction as defined in the vector of (1). The second track frame is the **geometric** Cartesian coordinate system. Both systems are linked by the digital map and define a track point. The geometric track coordinate system axes are along-track, cross-track and down. The track attitude is defined by right-handed Euler angles pitch as slope (θ), roll as bank (ϕ) and yaw as heading (ψ) between the navigation frame and the track frame. According to the angle definitions, a positive slope angle is defined as uphill, a positive bank angle is leaning to the right and a positive heading angle is defined clockwise from north. The direction cosine matrix (DCM) for vector transformation from the track frame to the navigation frame (NED) is defined by the rotation matrices of the angles ψ, θ and ϕ in [8]:

$$C_{\text{track}}^{\text{nav}} = \begin{pmatrix} c\theta c\psi & -c\phi s\psi + s\phi s\theta c\psi & s\phi s\psi + c\phi s\theta c\psi \\ c\theta s\psi & c\phi c\psi + s\phi s\theta s\psi & -s\phi c\psi + c\phi s\theta s\psi \\ -s\theta & s\phi c\theta & c\phi c\theta \end{pmatrix}. \tag{2}$$

The s and c in the rotation matrix refer to sine and cosine. The transformation from NED to the track frame is:

$$C_{\text{nav}}^{\text{track}} = C_{\text{track}}^{\text{nav}\top}. \tag{3}$$

The rotation axes of the turn velocities $\dot{\phi}$, $\dot{\theta}$ and $\dot{\psi}$ are defined in the following way: The $\dot{\phi}$ axis is the along-track axis in the horizontal plane, $\dot{\theta}$ the one to the cross-track axis and $\dot{\psi}$ is aligned with the down axis (see Fig. 1).

*4) **Train Frame**:* The train frame is a Cartesian coordinate system with x running along track, y cross the track and z down, and defined at a train axle in order to follow the shape of the track. It is possible to have multiple train frames for every wheel set. The train frame is directly dependent on the track frame. If the train is aligned with a positive track definition ($dir = 1$), the position, axes and attitude angles are the same as in the track system. If the train is aligned in opposite direction ($dir = -1$), the sign of the attitude angles changes as well as the axes x and y. The train motion is defined in the x-axis

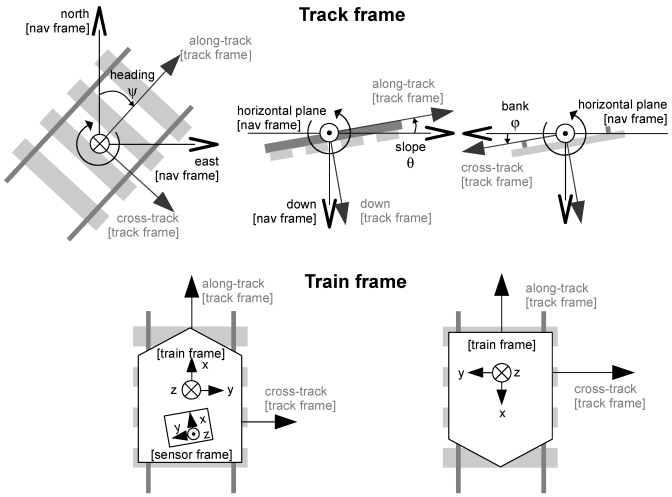

Fig. 1. [Top] Track frame and navigation frame (NED). [Bottom] Train frame, track frame and sensor frame.

of the train frame. The direction dir rotates the train frame in the same way as the track frame:

$$C_{\text{train}}^{\text{track}} = C_{\text{track}}^{\text{train}} = \begin{pmatrix} dir & 0 & 0 \\ 0 & dir & 0 \\ 0 & 0 & 1 \end{pmatrix}. \tag{4}$$

*5) **Sensor Frame**:* A sensor frame defines the attitude and position of a sensor relative to the train frame. Ideally the sensor is placed and aligned by the train frame definition.

C. Track Topology

Tracks are connected by switches, crossings or diamond switch crossings. A track R is defined between connections, i.e. it contains no switch or crossing. This definition ensures, that a track R is always true one-dimensional with no other access than the track begin or track end. A switch connects three tracks, a crossing four tracks. According to the travel direction and switch way position, a track splits up into two other tracks when passing a switch facing and two tracks merge into one track by passing trailing.

D. Track Geometry

Railway tracks are fixed to the earth, so any position on the tracks represent as well an absolute geographic position. The geometry of a track at a certain position is given by the attitude and the changes of the attitude over position. The track attitude contains heading ψ, bank ϕ and slope θ. Bank $\phi(s)$ is the lateral inclination and used in curves to compensate the lateral centripetal acceleration effects in curves. The bank angle is limited by restrictions to safety and passenger comfort. The bank of a track changes continuously by a ramp or a similar transition and is called bank change $\frac{d\phi(s)}{ds}$. Slope $\theta(s)$ is the inclination along a track and can be ascent or decent for changing altitude level. The slope change $\frac{d\theta(s)}{ds}$ is continuously and the slope is also limited. As an example for limits in German railroads, maximum bank angle is about 7° and the maximum slope angle is about 2.3° [9]. The change of the heading over the track position is curvature $\frac{d\psi(s)}{ds}$.

E. Inertial Sensing of 3D Track Geometry

A train is forced to follow the designated geographic track positions and geometric track attitude due to the track constrains. When the train moves with a velocity $\dot{s}$, the changes of the track attitude cause a rotation and a turn velocity of the train at certain track position s:

$$\dot{\phi} = \frac{d\phi}{dt} = \frac{d\phi}{ds}\frac{ds}{dt} = \frac{d\phi}{ds}\dot{s}, \tag{5}$$

$$\dot{\theta} = \frac{d\theta}{ds}\dot{s}, \tag{6}$$

$$\dot{\psi} = \frac{d\psi}{ds}\dot{s}. \tag{7}$$

As seen from these equations, the train turns only while it is moving ($\dot{s} \neq 0$). The accelerations of a train are caused by the train traction, a curved motion and the gravity vector dependent to the attitude of the train. First, the along-track train acceleration by the train traction is $\ddot{s}$ and measured exclusively by a_x. Second, the gravity acceleration g is dependent to the inclination by slope and bank angles and is calculated by the conversion of (3). Third, centripetal accelerations occur while the train is moving with velocity $\dot{s}$ in curves. There are two types of centripetal acceleration due to the horizontal curvature and due to the vertical slope change in crests or sags. The centripetal accelerations are orthogonal to the motion direction and turn axis and so measured by the y and z train axis, dependent to the bank angle. The full accelerations equations contains all three types:

$$a^x = \ddot{s} + g\sin\theta, \tag{8}$$

$$a^y = -g\sin\phi\cos\theta + \dot{\psi}\dot{s}\cos\phi - \dot{\theta}\dot{s}\sin\phi, \tag{9}$$

$$a^z = -g\cos\phi\cos\theta - \dot{\psi}\dot{s}\sin\phi - \dot{\theta}\dot{s}\cos\phi. \tag{10}$$

The Coriolis acceleration while a train moves over the earth is neglected due to the small amount. The train's turn velocities (ω^x, ω^y and ω^z) are also expressed in the train frame [8]:

$$\omega^x = \dot{\phi} - \dot{\psi}\sin\theta, \tag{11}$$

$$\omega^y = \dot{\theta}\cos\phi + \dot{\psi}\sin\phi\cos\theta, \tag{12}$$

$$\omega^z = \dot{\psi}\cos\theta\cos\phi - \dot{\theta}\sin\phi. \tag{13}$$

The earth rotation is neglected. The measurements are dependent to the velocity of the train, attitude and turn velocities which can be derived with (5–7) from changes of the attitude of the track.

F. Railway Switch

A switch connects one railway track with two other tracks. These two tracks differ in geometric characteristics, i.e. they urge in different ways on a train, which can be measured and used for localization. A standard switch has one straight track and one turning track. The radius or curvature of the turning track characterizes the standard switch and limits as well the velocity of a train moving over that switch. Table I shows a list of some standard switch examples used in Germany [9] showing the curvature, the angle of heading change and the arc length of the curved part of the switch: Switch way iden-

TABLE I
BASIC DESIGNS OF GERMAN STANDARD SWITCHES

radius	**curvature**	**switch angle**	**arc length**	**velocity**
r	$\frac{d\psi}{ds} = \frac{1}{r}$	α ($\tan\alpha$)	l	$v_{\max}$
[m]	[10^{-3} 1/m]	[°] [ratio]	[m]	[km/h]
190	5.26	6.3 (1:9)	21.049	40
		7.6 (1:7.5)	25.227	
300	3.33	4.1 (1:14)	21.403	50
		6.3 (1:9)	33.234	
500	2.00	4.8 (1:12)	35.670	60
		4.1 (1:14)	41.597	
760	1.32	3.1 (1:18.5)	41.053	80
		4.1 (1:14)	54.219	
1200	0.83	3.1 (1:18.5)	64.820	100
2500	0.40	2.2 (1:26.5)	94.307	120

tification is a critical process in railway navigation, especially if the tracks are parallel after passing the switch facing. It is possible to measure certain geometric characteristics of a track with an IMU when the train is moving. The turning track of a switch on a horizontal plane causes a turn rate $\dot{\psi}$ according to (7) and a cross-track centripetal acceleration a_k^{cross} due to the curvature $\frac{d\psi}{ds}$ of the track and the train speed $\dot{s}$:

$$a^{\text{cross}} = \frac{d\psi}{ds} \cdot \dot{s}^2. \tag{14}$$

For the horizontal case (9) and (14) are the same. Fig. 2 shows ideal turn rates of the switch examples over velocity calculated with (7). The turn rates decrease for larger switches moving

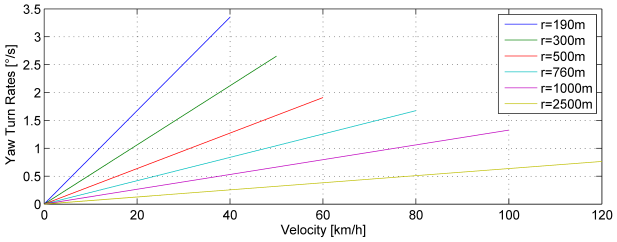

Fig. 2. Yaw turn rates of standard switch radiuses.

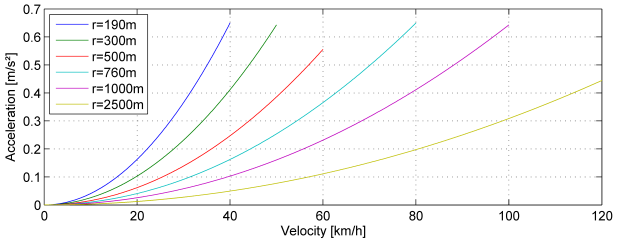

Fig. 3. Cross-track centripetal accelerations of standard switch radiuses.

with the maximal accepted velocity. Fig. 3 shows the centripetal acceleration dependent on the radius and the velocity calculated with (14). Here, the accelerations of the different switches are almost the same around 0.6 m/s^2 compared each with its maximal accepted velocity. If a train is moving with a low constant velocity, switches with large radiuses cause a low turn rate and acceleration. An IMU has a limited resolution due to noise and drift which depends of the IMU type. These facts have negative consequences on the accuracy of track precise localization methods. On the other hand, larger radiuses have larger arc length, as seen from table I. This relation causes more observations with a fixed measurement frequency and this has a positive effect for the convergence of the track precise localization methods.

III. TRAIN LOCALIZATION MODEL

A. Train State

We define a train state P_k, which contains a discrete data set indexed by the discrete time step k. The data is topological pose P_k^{topo}, geographic position P_k^{geo}, the 3D attitude P_k^{att} by the attitude angels (ϕ_k, θ_k, ψ_k) and P_k^{turn} is the turn velocity of the train ($\dot{\phi}_k$, $\dot{\theta}_k$, $\dot{\psi}_k$). The train state is:

$$\begin{aligned}\text{P}_k =&\{\text{P}_k^{\text{topo}}, \text{P}_k^{\text{geo}}, \text{P}_k^{\text{att}}, \text{P}_k^{\text{turn}}\} = \\ &\{R_k, s_k, dir_k, lat_k, long_k, alt_k, \phi_k, \theta_k, \psi_k, \dot{\phi}_k, \dot{\theta}_k, \dot{\psi}_k\}.\end{aligned} \tag{15}$$

B. Train Motion Transition

The train motion is one-dimensional due to constrains of the rail tracks and we define the motion state U_k by along track acceleration $\ddot{s}_k$, velocity $\dot{s}_k$ and a traveled distance Δs_k in the time between $k-1$ and k:

$$\text{U}_k = (\Delta s_k, \dot{s}_k, \ddot{s}_k)^\top. \tag{16}$$

The train motion model computes the transition in the time between $k-1$ and k of Δs_k, $\dot{s}_k$, $\ddot{s}_k$ and the process noise n_{k-1}^{proc}. The motion transition function f_{motion} is defined by:

$$\text{U}_k = f_{\text{motion}}(\text{U}_{k-1}) + n_{k-1}^{\text{proc}} = \begin{pmatrix} \dot{s}_{k-1}\Delta t + \ddot{s}_{k-1}\frac{\Delta t^2}{2} \\ \dot{s}_{k-1} + \ddot{s}_{k-1}\Delta t \\ \ddot{s}_{k-1} \end{pmatrix} + n_{k-1}^{\text{proc}}. \tag{17}$$

Further, the output of this train motion model is limited by train specific parameters, such as maximum velocity, acceleration and deceleration.

C. Digital Map

The digital map contains position relevant information for the localization procedure. The map contains information of topological, geographic and track geometric data and further information about the track net, track IDs, connections like switches or crossings and dead endings. The position of a train standing on a certain track can be described either by topological or geographic position. A reasonable representation for railway navigation is the topological coordinate frame. As most sensors cannot directly measure in the topological system, the map contains additionally geographic and geometric track representation. The geographic and geometric information of a particular position is provided by the digital map and referenced by the topological pose:

$$\left.\begin{matrix}\text{geographic track position} \\ \text{track geometry}\end{matrix}\right\} = f_{\text{map}}(\text{P}_k^{\text{topo}}). \tag{18}$$

In practice, the map is organized by a list of tracks. Every track contains a unique track ID R, connections and track data

parametrized to one-dimensional position s on the track. The geographic and geometric track data is stored by supporting points of any kind of continuous graph representation. There are many methods of representing a continuous function by discrete points. The simplest might be the polygonal line approximation, which interconnects points with lines. More advanced methods for the geographic track representation use spline approximations [13].

D. Transition Model

Trains move exclusively on railway tracks. The digital map contains information about these tracks and therefore the transition model includes the map. A train state transition happens at every time step k in the topological coordinate frame. The new topological pose $\mathrm{P}_k^{\text{topo}}$ is calculated from the previous pose $\mathrm{P}_{k-1}^{\text{topo}}$ and the traveled distance Δs_k:

$$\mathrm{P}_k^{\text{topo}} = f_{\text{map}}(\mathrm{P}_{k-1}^{\text{topo}}, \Delta s_k). \tag{19}$$

At any switch passing facing for example, the transition gets nonlinear and splits in two possibilities. Afterwards, the remaining train states are updated with information from the digital map:

$$\{\mathrm{P}_k^{\text{geo}}, \mathrm{P}_k^{\text{att}}, \mathrm{P}_k^{\text{turn}}\} = f_{\text{map}}(\mathrm{P}_k^{\text{topo}}, \dot{s}_k). \tag{20}$$

The turn velocities $\mathrm{P}_k^{\text{turn}}$ are calculated by the track geometry and the train velocity with (5–7). Equations (19) and (20) are combined to one map transition function:

$$\mathrm{P}_k = f_{\text{map}}(\mathrm{P}_{k-1}, \mathrm{U}_k). \tag{21}$$

E. Measurement Models

1) GNSS: The GNSS measures the geographic train positions. The antenna may be mounted on the roof of a train with a distance vector $\vec{d}$ (train frame) which is normal to the track plane, along track to the IMU and cross-track to the track center line. The measurements Z^{GNSS} and P^{geo} from the map are translated by the earth frame conversion in the navigation frame. (2) and (4) convert $\vec{d}$ in the navigation frame:

$$h_{\text{GNSS}} = C_{\text{earth}}^{\text{nav}}(\mathrm{P}_k^{\text{geo}}) + C_{\text{track}}^{\text{nav}} C_{\text{train}}^{\text{track}} \cdot \vec{d}^{\,\text{train}}. \tag{22}$$

The GNSS sensor model with the sensor noise n^{GNSS} is:

$$\mathrm{Z}_k^{\text{GNSS}} = h_{\text{GNSS}}(\mathrm{P}_k^{\text{geo}}, \mathrm{P}_k^{\text{att}}, \vec{d}) + n_k^{\text{GNSS}}. \tag{23}$$

2) IMU: The IMU is placed near the train mass center and aligned with the train frame axes. A calibration transformation $C_{\text{IMU}}^{\text{train}}$ must be applied for other alignment. The IMU measures accelerations caused by the train traction, a curved motion and the gravity vector. The translative train motion acceleration is corrected by the gravity measurement for slope angles $\neq 0$ and calculated by (8):

$$\ddot{s} = a_x + g \sin\theta. \tag{24}$$

As the inertial data of a_x is used to measure train motion, the inertial data of a_y, a_z and the turn rates are used to measure the influence of the track geometry:

$$\mathrm{Z}_k^a = h_a(\mathrm{P}_k^{\text{att}}, \mathrm{P}_k^{\text{turn}}, \dot{s}_k) + n_k^a, \tag{25}$$

$$\mathrm{Z}_k^\omega = h_\omega(\mathrm{P}_k^{\text{att}}, \mathrm{P}_k^{\text{turn}}) + n_k^\omega. \tag{26}$$

The measurement equations h_{a_y} and h_{a_z} are presented in (9–10) and the turn rates equations h_{ω_x}, h_{ω_y} and h_{ω_z} are defined in (11–13).

IV. Probabilistic Train Localization

A probabilistic approach computes the estimates of the train state $\mathbf{P}_k$, which contains all states a train can take at the time step k. We denote $\mathbf{U}_k$ as the one dimensional train motion. The sensor measurements of time k are described by $\mathbf{Z}_k$ and $\mathbf{E}_k$ are measurement errors which are persistent over at least two time steps. Examples are multipath errors of the GNSS, drift of inertial sensors, calibration errors and wheel slip of the odometer or feature sensors. White Gaussian sensor noise is independent over time and not part of $\mathbf{E}_k$. Finally, the physical railway environment including the track network is time invariant and denoted by $\mathbf{M}$. The bold notation of the variables represents a random variable.

A. Localization Posterior

The probabilistic localization posterior is the estimation of all train states over time $\mathbf{P}_{0:k}$, all train motions $\mathbf{U}_{0:k}$ and all measurement errors $\mathbf{E}_{0:k}$ given all measurements $\mathbf{Z}_{1:k}$ and the track network $\mathbf{M}$:

$$p(\mathbf{P}_{0:k}, \mathbf{U}_{0:k}, \mathbf{E}_{0:k} | \mathbf{Z}_{1:k}, \mathbf{M}). \tag{27}$$

This posterior is computed by a sequential Bayesian filter.

B. Dynamic Bayesian Network

A dynamic Bayesian network (DBN) visualizes causal dependencies of effects in a directed acyclic graph. In Fig. 4 we draw the DBN for two time steps of a train, which is equipped with erroneous sensors and the causal dependencies are shown by pointers. From the DBN we can see, that the

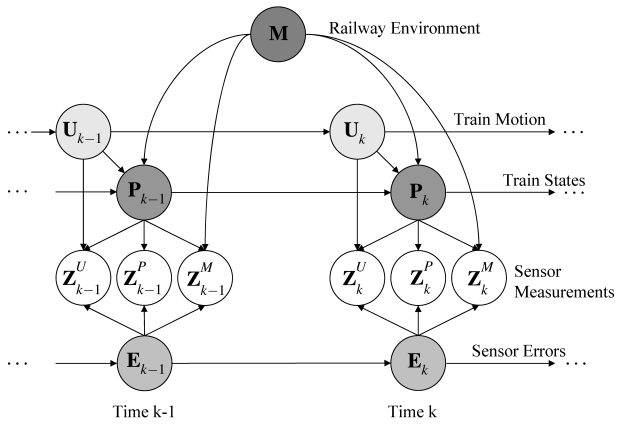

Fig. 4. Dynamic Bayesian network.

train state $\mathbf{P}_k$ is directly dependent to the last train state $\mathbf{P}_{k-1}$, the 1D train motion $\mathbf{U}_k$ and the railway environment $\mathbf{M}$. The railway environment is time invariant and has a strong influence on the train states caused by the tracks. The dependency of $\mathbf{P}_k$ to $\mathbf{P}_{k-1}$ and $\mathbf{U}_k$ to $\mathbf{U}_{k-1}$ can be explained by physical effects. A train can not change its position, speed

or attitude randomly between two time steps because of the inertia of train mass and limited speed, acceleration and turn rates. The train has onboard sensors for localization purposes, which measure physical characteristics of the train states. The measurements $\mathbf{Z}_k$ are directly dependent to the train states $\mathbf{P}_k$ and independent from the last measurements. $\mathbf{Z}_k$ is split into three different groups: $\mathbf{Z}_k^{\mathrm{U}}$, $\mathbf{Z}_k^{\mathrm{P}}$ and $\mathbf{Z}_k^{\mathrm{M}}$.

$\mathbf{Z}_k^{\mathrm{U}}$ is dependent to train motion, the train state and to sensor errors and refers to the acceleration and turn rate measurements by the IMU ($\mathbf{Z}^{\mathrm{IMU}}$) and to velocity measurements by the odometer ($\mathbf{Z}^{\mathrm{odo}}$). Dependent sensor errors $\mathbf{E}^{\mathrm{IMU}}$ are e.g. biases due to calibration errors or drift and $\mathbf{E}^{\mathrm{odo}}$ are calibration errors or wheel slip.

$\mathbf{Z}_k^{\mathrm{P}}$ is dependent on the train state and the sensor errors. Typical sensors are position sensors such as GNSS ($\mathbf{Z}^{\mathrm{GNSS}}$) and the dependent errors ($\mathbf{E}^{\mathrm{GNSS}}$) are multipath errors for instance. With the fact that the train is dependent on the railway environment or tracks respectively, the railway environment will have some influence on these measurements through the train states. $\mathbf{Z}_k^{\mathrm{P}}$ and $\mathbf{Z}_k^{\mathrm{U}}$ are independent of $\mathbf{M}$ and measure $\mathbf{P}_k$ and $\mathbf{U}_k$ directly.

Measurements $\mathbf{Z}_k^{\mathrm{M}}$ are additionally dependent on the railway environment. The feature sensors like camera or the eddy current sensor measure features directly in the railway environment with a different position than the train. These sensors are as well dependent to the train position to be near enough to the feature i.e. within the sensing distance.

C. General factorized localization posterior

In a previous work [14], we derived the factorized solution of the localization posterior:

$$\begin{aligned} &p(\{\mathbf{PUE}\}_{0:k}|\mathbf{Z}_{1:k},\mathbf{M}) \propto \\ &\underbrace{p(\mathbf{Z}_k^{\mathrm{M}}|\{\mathbf{PE}\}_k,\mathbf{M})\cdot p(\mathbf{Z}_k^{\mathrm{P}}|\{\mathbf{PE}\}_k)\cdot p(\mathbf{Z}_k^{\mathrm{U}}|\{\mathbf{PUE}\}_k)}_{\text{sensor likelihoods}}\cdot \\ &\underbrace{p(\mathbf{U}_k|\mathbf{U}_{k-1})}_{\text{1D motion model}}\cdot\underbrace{p(\mathbf{P}_k|\mathbf{P}_{k-1},\mathbf{U}_k,\mathbf{M})}_{\text{train state transition}}\cdot \\ &\underbrace{p(\mathbf{E}_k|\mathbf{E}_{k-1})}_{\text{sensor errors transition}}\cdot\underbrace{p(\{\mathbf{PUE}\}_{0:k-1}|\mathbf{Z}_{1:k-1},\mathbf{M})}_{\text{recursion}}. \end{aligned} \tag{28}$$

The factorized solution is proportional ($\propto$) to the posterior, because of a missing normalization factor, which is computed separately. The factorization is necessary to be able to calculate the posterior in a Bayesian filter. In the next chapter, a particle filter is implemented to compute the posterior.

V. Particle Filter Implementation

For the Bayesian filter implementation we choose a particle filter for the estimation problem of the posterior (27), because of the discrete distribution of the tracks. As described in [15], particle filter represents probability density functions by appropriate particle distributions with appropriate weights of N_p particles. The posterior of (27) is represented by

$$p(\{\mathbf{PUE}\}_{0:k}|\mathbf{Z}_{1:k},\mathbf{M}) \approx \{x_{0:k}^i, w^i\}_{i=1}^{N_p}, \tag{29}$$

where $x_{0:k}^i$ is the i-th particle with its weight w^i of N_p particles and $x_{0:k}^i$ is one sample of the posterior of all time steps until k. Particles are generated from a function which is easy to calculate [15], called the proposal function:

$$x_{0:k}^i \sim q(\{\mathbf{PUE}\}_{0:k}|\mathbf{Z}_{1:k},\mathbf{M}). \tag{30}$$

Afterwards these particles are weighted [15]. The weights are proportional to the fraction posterior over proposal function:

$$w_k \propto \frac{p(\{\mathbf{PUE}\}_{0:k}|\mathbf{Z}_{1:k},\mathbf{M})}{q(\{\mathbf{PUE}\}_{0:k}|\mathbf{Z}_{1:k},\mathbf{M})}. \tag{31}$$

A. Recursive Proposal Density

The proposal density is practically generated and sampled to obtain the particle distribution. Further, a proposal density in recursive factorization is desired:

$$\begin{aligned} q(\{\mathbf{PUE}\}_{0:k}|\mathbf{Z}_{1:k},\mathbf{M}) =& q(\{\mathbf{PUE}\}_k|\{\mathbf{PUE}\}_{0:k-1},\mathbf{Z}_{1:k},\mathbf{M})\cdot \\ & q(\{\mathbf{PUE}\}_{0:k-1}|\mathbf{Z}_{1:k-1},\mathbf{M}) \end{aligned} \tag{32}$$

Now, we design the proposal function. We are free to choose any method of spreading particles in our domain. If we choose badly, there would be too less or even no particles near the actual truth. It is possible to incorporate measurements by sampling from its likelihood function [15]. We define ($\hat{=}$) for the first factor of (32):

$$\begin{aligned} q(\{\mathbf{PUE}\}_k|\{\mathbf{PUE}\}_{0:k-1},\mathbf{Z}_{1:k},\mathbf{M}) \hat{=}& p(\mathbf{E}_k|\mathbf{E}_{k-1})\cdot \\ & p(\mathbf{U}_k|\mathbf{Z}_k^{\mathrm{U}},\mathbf{P}_k)\cdot p(\mathbf{U}_k|\mathbf{U}_{k-1})\cdot p(\mathbf{P}_k|\mathbf{P}_{k-1},\mathbf{U}_k,\mathbf{M}). \end{aligned} \tag{33}$$

$p(\mathbf{E}_k|\mathbf{E}_{k-1})$ is the sensor error process model and calculates the transition of an error of one time step. The train acceleration $\ddot{s}$ is sampled from a Gaussian measurement distribution ($\mathcal{N}(\text{argument}|\text{mean},\text{covariance})$) of the along-track acceleration measurement. Z^{a_x} is corrected by (24) and the measurement variance is σ_a^2 due to the sensor noise:

$$\begin{aligned} \ddot{s}_k^{\ i} \sim& p(\mathbf{U}_k^{\ddot{s}}|\mathbf{Z}_k^{a_x},\mathbf{P}_k^{\mathrm{att}}) = \\ & \mathcal{N}(\ddot{s}^{\ i}|Z_k^{a_x}+g\sin(\theta),\sigma_a^2). \end{aligned} \tag{34}$$

$p(\mathbf{U}_k|\mathbf{U}_{k-1})$ is the one-dimensional motion model and computes the distance Δs and velocity $\dot{s}$ from the sampled acceleration and (17). The transition $p(\mathbf{P}_k|\mathbf{P}_{k-1},\mathbf{U}_k,\mathbf{M})$ is computed by (21) with the previous topological position, train motion and the map. When a particle arrives at a switch, the switch way with the continuing track ID is randomly selected. Despite from this general transition model, the map in our approach contains no uncertainty. Therefore the map is not described with a random variable (**M**=M). Finally, the proposal function with along-track acceleration and ideal map is:

$$\begin{aligned} q(\{\mathbf{PUE}\}_{0:k}|\mathbf{Z}_{1:k},\mathrm{M}) \hat{=}& p(\mathbf{U}_k^{\ddot{s}}|\mathbf{Z}_k^{a_x},\mathbf{P}_k^{\mathrm{att}})\cdot p(\mathbf{U}_k|\mathbf{U}_{k-1})\cdot \\ & p(\mathbf{E}_k|\mathbf{E}_{k-1})\cdot p(\mathbf{P}_k|\mathbf{P}_{k-1},\mathbf{U}_k,\mathrm{M})\cdot \\ & \underbrace{q(\{\mathbf{PUE}\}_{0:k-1}|\mathbf{Z}_{1:k-1},\mathrm{M})}_{\text{recursion}} \end{aligned} \tag{35}$$

B. Particle Weights Update

The particle weights are derived from (31), in which the general posterior (28) is divided by the proposal function (35):

$$w_k \propto \frac{p(\mathbf{Z}_k^{\mathrm{M}}|\{\mathbf{PE}\}_k, \mathrm{M}) \cdot p(\mathbf{Z}_k^{\mathrm{P}}|\{\mathbf{PE}\}_k) \cdot p(\mathbf{Z}_k^{\mathrm{U}}|\{\mathbf{PUE}\}_k)}{p(\mathbf{U}_k|\mathbf{Z}_k^{\mathrm{U}})} \cdot \frac{p(\mathbf{U}_k|\mathbf{U}_{k-1}) \cdot p(\mathbf{E}_k|\mathbf{E}_{k-1}) \cdot p(\mathbf{P}_k|\mathbf{P}_{k-1}, \mathbf{U}_k, \mathrm{M})}{p(\mathbf{U}_k|\mathbf{U}_{k-1}) \cdot p(\mathbf{E}_k|\mathbf{E}_{k-1}) \cdot p(\mathbf{P}_k|\mathbf{P}_{k-1}, \mathbf{U}_k, \mathrm{M})} \cdot \underbrace{\frac{p(\{\mathbf{PUE}\}_{0:k-1}|\mathbf{Z}_{1:k-1}, \mathrm{M})}{q(\{\mathbf{PUE}\}_{0:k-1}|\mathbf{Z}_{1:k-1}, \mathrm{M})}}_{\text{recursion} = w_{k-1}} \tag{36}$$

Finally the weight is computed recursively of the previous weight, the 1D motion model and the sensor likelihoods of GNSS, IMU and optional feature sensor:

$$w_k \propto w_{k-1} \cdot p(\mathbf{Z}_k^{\text{feature}}|\mathbf{P}_k, \mathbf{E}_k^{\text{feature}}, \mathrm{M}) \cdot p(\mathbf{Z}_k^{\text{GNSS}}|\mathbf{P}_k, \mathbf{E}_k^{\text{GNSS}}) \cdot p(\mathbf{Z}_k^{\text{IMU}}|\mathbf{P}_k, \mathbf{U}_k, \mathbf{E}_k^{\text{IMU}}). \tag{37}$$

C. Sensor Likelihoods

The sensor likelihood function calculates how likely a measurement fits to the estimation. Our generic likelihood function is modeled by a Gaussian distribution and applied to the state of the i'th particle:

$$p(\mathbf{Z}_k|\{\mathbf{PUE}\}_k = \{\mathrm{PUE}\}_k^i) \hat{=} \mathcal{N}\left(h(\{PUE\}_k^i)\middle|Z_k, \Sigma_Z\right), \tag{38}$$

in which $h(P_k^i, U_k^i, E_k^i)$ is the measurement equation calculated by train pose and train motion and sensor errors. Z_k is the measurement and Σ_Z is the covariance due to sensor noise. We define the likelihood of the GNSS measurement in the navigation frame:

$$p(\mathbf{Z}_k^{\text{GNSS}}|\{\mathrm{PE}\}_k^i) \hat{=} \mathcal{N}\left(h_{\text{GNSS}}(P_k^{i,\text{geo,att}}, \vec{d})\middle|C_{\text{earth}}^{\text{nav}}(\mathrm{Z}_k^{\text{GNSS}}), \Sigma_{\text{GNSS}}\right). \tag{39}$$

The sensor model of IMU acceleration measurements a_y and a_z is for every i'th particle:

$$p(\mathbf{Z}_k^a|\{\mathrm{PUE}\}_k^i) \hat{=} \mathcal{N}\left(h_a(P_k^{i,\text{turn,att}}, \dot{s}_k{}^i)\middle|Z_k^a, \sigma_a^2\right), \tag{40}$$

in which h_{a_y} is (9) and h_{a_z} is (10). The turn rate sensor likelihood is for every i'th particle:

$$p(\mathbf{Z}_k^\omega|\{\mathrm{PUE}\}_k^i) \hat{=} \mathcal{N}\left(h_\omega(P_k^{i,\text{turn,att}}, \dot{s}_k{}^i)\middle|Z_k^\omega, \sigma_\omega^2)\right). \tag{41}$$

in which the measurement models h_{ω_x},h_{ω_y} and h_{ω_x} are (11), (12) and (13). Finally, the weight function for the i'th particle with the IMU and GNSS likelihoods is:

$$w_k^i \propto w_{k-1}^i \cdot p(\mathbf{Z}_k^{\text{GNSS}}|\{\mathrm{PE}\}_k^i) \cdot p(\mathbf{Z}_k^{\omega_x}|\{\mathrm{PUE}\}_k^i) \cdot p(\mathbf{Z}_k^{\omega_y}|\{\mathrm{PUE}\}_k^i) \cdot p(\mathbf{Z}_k^{\omega_z}|\{\mathrm{PUE}\}_k^i) \cdot p(\mathbf{Z}_k^{a_y}|\{\mathrm{PUE}\}_k^i) \cdot p(\mathbf{Z}_k^{a_z}|\{\mathrm{PUE}\}_k^i). \tag{42}$$

VI. Algorithm Summary

1) Initialize all N_p particles to $\mathrm{U}_0^i = (0,0,0)^\top$, all $\mathrm{E}_0^i = 0$ and $\mathrm{P}_0^{i,\text{topo}}$ to a suitable initial distribution and get the remaining pose from the map $\mathrm{P}_k^i = f_{\text{map}}(\mathrm{P}_0^{i,\text{topo}}, 0)$.
2) For every time step k:
   a) Draw samples from the train acceleration according to (34) and assign it to N_p particles.
   b) Compute train motion U_k^i by (17) with the sampled acceleration.
   c) Compute train state $\mathrm{P}_k^i = f_{\text{map}}(\mathrm{P}_{k-1}^{i,\text{topo}}, \mathrm{U}_k^i)$ from the previous topological pose, train motion and the known map.
   d) If available, compute for all errors the transitions $p(\mathrm{E}_k^i|\mathrm{E}_{k-1}^i)$.
   e) Weight all N_p particles according to (42).
   f) If feature measurements are available, weight with $p(\mathbf{Z}_k^{\text{feature}}|\mathbf{P}_k^{\text{topo}}, \mathbf{E}_k^{\text{feature}}, \mathrm{M})$.
   g) Perform resampling if necessary.

A suitable initialization distribution of 1) is either a uniform distribution of topological positions over the entire track network or the particles are initialized on tracks in a certain vicinity of the first GNSS position measurement.

VII. Proof of Concept

Fig. 5 shows a critical track network scenario by parallel tracks with a distance of $4\mathrm{m}$ after the switch A with the design parameters of the first switch of table I. The train moves from track R_1 over R_2 to R_4 with a velocity of $40^{\mathrm{km}}/_{\mathrm{h}}$. Particles

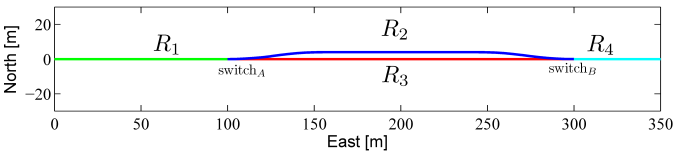

Fig. 5. Parallel track network scenario with four different tracks.

are initialized on all tracks with track positions from a uniform distribution and all directions assuming no initial knowledge about the position. This simulation assumes a Gaussian model of the GNSS measurements with a standard deviation of $4\mathrm{m}$ at a data rate of $1\mathrm{Hz}$ in order to show the effects of parallel track distance and deviations in the same range. The acceleration sensor noise is $0.05^{\mathrm{m}}/_{\mathrm{s}^2}$ and the gyroscope sensor noise is $0.5^{\circ}/_{\mathrm{s}}$ with a data rate of $10\mathrm{Hz}$.

A. Localization with GNSS only

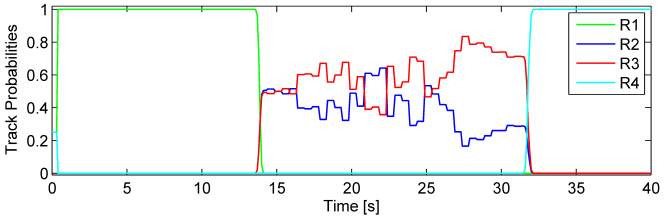

Fig. 6. Track probabilities for GNSS only.

Fig. 6 shows the estimation result of the localization algorithm by track probabilities, in which only the GNSS provides data. The train reaches the switch A after about 13s and the particles split up on both tracks R_2 and R_3 with equal probability. The noisy GNSS position measurements can not supply enough information to resolve the correct track R_2.

B. Enabled inertial sensing of track geometry

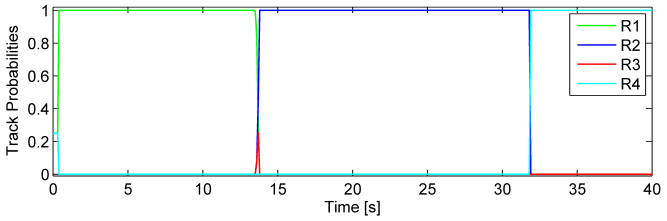

Fig. 7. Track probabilities for GNSS and enabled inertial.

1) GNSS with inertial track geometry observations: Fig. 7 shows the resulting track probabilities with GNSS and IMU measuring the effects of the track geometry on the train. The result shows a quick convergence to the correct track R_2. Some particles in front of the train propose positions on track R_3 before the train reaches the switch and the curved arc. These particles are at first awarded by the IMU likelihood function being on a straight but as soon as the train starts turning and cross-track acceleration occurs, the probability of R_3 decreases correctly.

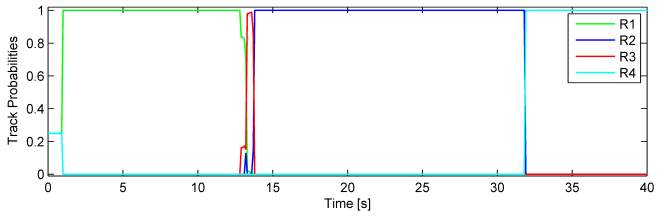

Fig. 8. Enabled inertial and GNSS signal lost after 2s.

2) Enabled inertial, but less GNSS availability: Fig. 8 shows the localization probabilities when the GNSS is not providing any measurements after 2s. The track probabilities show less optimal result at $13s$ when the incorrect track R_3 is estimated with the highest probability. The missing GNSS causes a larger particle spread with significant weights along the track. Particles in front of the truth and on the straight track are again awarded by the IMU likelihoods. When the true train turns on R_2, the filter resolves to the correct track.

C. Results

GNSS position measurements have a strong benefit in initializing and the update of position and motion related estimates. On single track scenarios, GNSS solves the track selective demand because of the very large distances to other tracks compared to a mean accuracy. In narrow parallel track scenarios, the GNSS does not provide enough information to resolve the track quickly, certain and stable. The inertial sensing of the 3D track geometry show a quick conversion to the correct track. Even in the case where no GNSS measurements are available, the filter estimates the correct track robustly.

VIII. Conclusions

We have presented a Bayesian approach for probabilistic train localization combining global navigation satellite system (GNSS) and inertial measurement unit (IMU) data and further sensor data. The IMU measurements are dependent on the train motion and 3D track geometry and are used for estimating a topological position in the track network with a non integrative method.

First simulations show a clear benefit in critical railway scenarios in terms of accuracy for track selective train localization. A combined approach increases also the robustness of a track selective positioning during GNSS outages.

As an outlook, a further increase of robustness is expected with the use of feature classification sensors, such as switch way detectors based on vision or eddy current. The digital map is considered to be ideal in this approach. We assume for the map a correct, complete and especially exact information source. Further work can also focus on an uncertain and incomplete map, among a simultaneous localization and mapping (SLAM) process for a map generation.

References

[1] T. Strang, M. Meyer zu Hoerste, and X. Gu, "A Railway Collision Avoidance System Exploiting Ad-hoc Inter-vehicle Communications and Galileo," in *13th World Congress on Intelligent Transportation Systems, London, UK*, 2006.

[2] O. Plan, "GIS-gestützte Verfolgung von Lokomotiven im Werkbahnverkehr," Ph.D. dissertation, University of German Federal Armed Forces Munich, Germany, 2003.

[3] F. Böhringer, "Gleisselektive Ortung von Schienenfahrzeugen mit bordautonomer Sensorik," Ph.D. dissertation, Universität Karlsruhe (TH), Germany, 2008.

[4] S. Hensel, C. Hasberg, and C. Stiller, "Probabilistic Rail Vehicle Localization With Eddy Current Sensors in Topological Maps," *Intelligent Transportation Systems, IEEE Transactions on*, vol. 12, no. 4, pp. 1525 –1536, dec. 2011.

[5] International Union of Railways, "RMTS - European Rail Management Traffic System," http://www.uic.org/spip.php?rubrique847.

[6] J. Wohlfeil, "Vision based rail track and switch recognition for self-localization of trains in a rail network," in *Intelligent Vehicles Symposium (IV), 2011 IEEE*, june 2011, pp. 1025 –1030.

[7] S. Saab, "A map matching approach for train positioning. I. Development and analysis," *Vehicular Technology, IEEE Transactions on*, vol. 49, no. 2, pp. 467 –475, mar 2000.

[8] D. Titterton and J. Weston, *Strapdown Inertial Navigation Technology, 2nd Edition*. The Institution of Electrical Engineers (IEE), 2004.

[9] H. Jochim and F. Lademann, *Planung von Bahnanlagen*. Carl Hanser Verlag München, Germany, 2009.

[10] P. Misra and P. Enge, *Global Positioning System: Signals, Measurements, and Performance*. Ganga-Jamuna Press, 2006.

[11] O. Heirich, A. Lehner, P. Robertson, and T. Strang, "Measurement and analysis of train motion and railway track characteristics with inertial sensors," in *Intelligent Transportation Systems (ITSC), 2011 14th International IEEE Conference on*, oct. 2011, pp. 1995 –2000.

[12] M. Malvezzi, B. Allotta, and M. Rinchi, "Odometric estimation for automatic train protection and control systems," *Vehicle System Dynamics*, vol. 49, no. 5, pp. 723–739, 2011.

[13] C. Hasberg and S. Hensel, "Bayesian mapping with probabilistic cubic splines," in *Machine Learning for Signal Processing (MLSP), 2010 IEEE International Workshop on*, 29 2010-sept. 1 2010, pp. 367 –372.

[14] O. Heirich, P. Robertson, A. Cardalda Garcia, T. Strang, and A. Lehner, "Probabilistic localization method for trains," in *Intelligent Vehicles Symposium (IV), 2012 IEEE*, june 2012.

[15] M. Arulampalam, S. Maskell, N. Gordon, and T. Clapp, "A tutorial on particle filters for online nonlinear/non-Gaussian Bayesian tracking," *Signal Processing, IEEE Transactions on*, vol. 50, no. 2, pp. 174 –188, feb 2002.